AUTRES COMMUNICATIONS

AÉRONOMIE SPATIALE

The interpretation of protons and electrons observations from ATS 6 satellite within the frame of McIlwain's electric field model

J. LEMAIRE (*)
Institut d'Aéronomie Spatiale de Belgique
Avenue Circulaire, 3
B-1180 Bruxelles, Belgium

Abstract. — The " E3H " electric field model has been deduced by McIlwain from dynamical proton and electron energy spectrograms measured along the geostationary orbit of ATS 5 satellite. It is shown that this empirical model, which has often been regarded with some reticence by a number of theoreticians, fits well with the measurements, also made in the equatorial region of the magnetosphere, onboard another geostationary satellite (ATS 6) during an extended period of time when the geomagnetic activity index K_p ranged between 1 and 2. This confirmation validates the E3H model, at least for such extended periods of time when $K_p = 1$ and 2+.

From the dynamical spectrograms of ATS 6 observed on 19 July 1974, some evidence for patchy or localized injection of a magnetosheath plasma cloud across the late afternoon local time sector of magnetopause has been gained.

INTRODUCTION

The E3H electric field distribution has been deduced by McIlwain [1972, 1974] from electron and proton energy spectra observed along the geostationary orbit of ATS 5 [Deforest and McIlwain, 1971].

Fig. 1 shows equatorial equipotential lines ($\phi = ct$) corresponding to McIlwain's electrostatic field. This electric field distribution has many features in common with the first magnetospheric convection

(*) Présenté par M. M. NICOLET.

electric field published in 1961 by Axford and Hines [1961]. Indeed in both models the gradient of the potential, ϕ, (or the electric field $\vec{E}$), has a large radial component in the post-midnight local time sector. Note also the significant dawn-dusk asymmetry in the equipotential contours. In both the E3H model and in Axford and Hines electrostatic field distribution, the last closed equipotential extends up to the magnetopause near 1800 LT; the last closed equipotential for the E3H model coïncides with the outer edge of the shaded zone of figure 1. Furthermore, there is no singular point where the electric field vanishes and consequently where the $E \times B/B^2$ drift velocity tends to zero (i.e. a stagnation point).

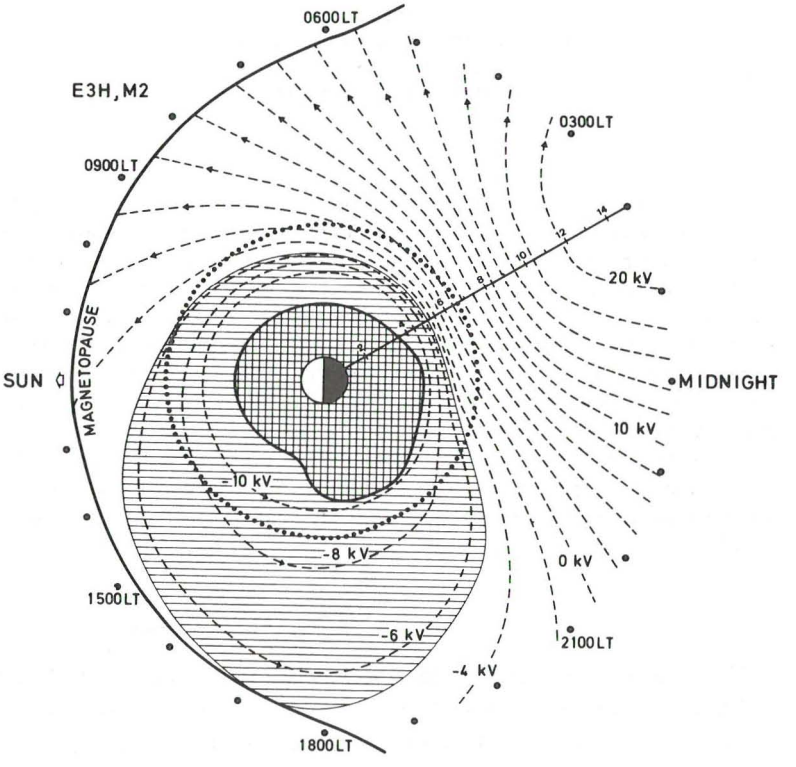

FIG. 1. — A contour plot of model E3H electric equipotential lines in the equatorial plane of the magnetosphere. The dashed lines are also streamlines (drift paths) of zero-energy protons and electrons. The last closed equipotential coïncides with the outer edge of the shaded area. This limit intersects the geostationary orbit (R = 6.6; shown by a dotted circle) at 2230 LT and 1044 LT. The position of the plasmapause as observed by Carpenter [1966] is shown by the solid line with a bulge at 1800 LT.

After the discovery of the plasmapause boundary by Carpenter [1963, 1966] and, after it had been found that this surface of discontinuity has a dawn-dusk asymmetry shown by the innermost shaded area in figure 1, a number of different mathematical models for the magnetospheric electric field have been proposed by many theoreticians [Brice, 1967 ; Kavanagh *et al.*, 1968 ; Volland, 1973 ; Stern, 1977 and others]. Figure 2 shows the equatorial cross section of equipotential surfaces for one of these mathematical models.

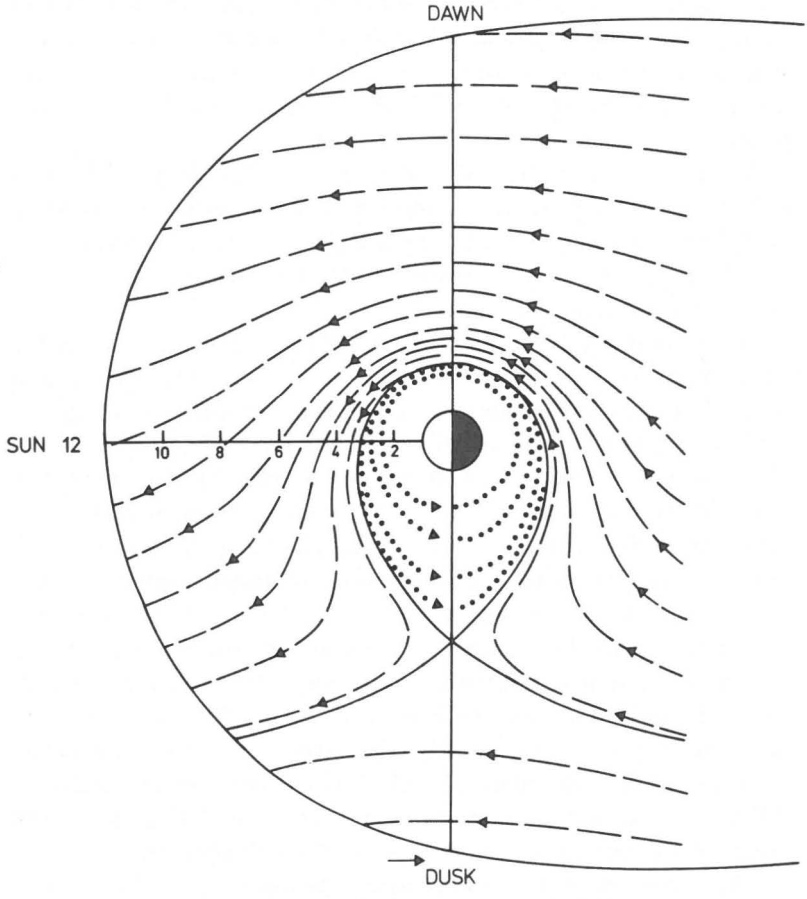

FIG. 2. — A contour plot of the uniform dawn-dusk electric field model by Kavanagh *et al.* [1968]. The last closed equipotential passing through the singular point at 1800 LT, is chosen to fit the equatorial position of the plasmapause. The dotted curves are also streamlines of electrons and ions confined within a region which has been identified with the plasmasphere, according to the MHD-theory for the plasmapause formation.

A common feature of all these theoretical models is that the last closed equipotential does not extend up to the magnetopause, as it does in the E3H model. The last equipotential in all these theoretical models is always chosen to coïncide with the observed positions of the plasmapause surface. Indeed, according to an early MHD theory by Brice [1967], the plasmapause should coïncide with the last closed equipotential surface of the magnetospheric electric field distribution ! Since the actual plasmapause does not extend up to the magnetopause, these latter modelers had to assume the existence of a singular point in their semi-empirical E-field models. Indeed, this mathematical singularity determines uniquely the position of the last closed equipotential and, according to the MHD theory, the position of the plasmapause.

When McIlwain [1972, 1974] deduced the E3H electric field from ATS 5 particle observations along geostationary orbit, his empirical model was criticized for not having a singular point, i.e. a point where the electric field becomes equal to zero, and, across which the last closed equipotential would pass.

It is mainly for this reason that the E3H electric field model has been widely disregarded, even though it is not simply a theoretical model but is based on electron and proton dynamical spectrograms directly observed in the magnetosphere, like that of figure 3a.

Meanwhile, an alternative theory was proposed for the formation of the plasmapause [Lemaire, 1975, 1976 ; Lemaire and Kowalkowski, 1981]. According to this new theory the plasmapause does not coïncide with the last closed equipotential of the magnetospheric electric field. Indeed, when the physical process of plasma interchange motion is included in the theory, a well defined plasmapause is continuously forming at finite radial distances in the magnetosphere, even for electric field distributions (like the E3H model) which have no mathematical singular point. Consequently, the main reason for disregarding empirical models, like those of Axford and Hines [1961] or McIlwain [1972, 1974], is no longer valid. Nevertheless, the E3H model is still being treated with some reserve by most of the theoreticians.

The aim of this article is to compare the model E3H with observations from another geostationary satellite (ATS 6), and to check whether or not it gives a realistic approximation to the actual distribution of electric fields in the equatorial region of the magnetosphere.

Spectrogram description

Figure 3a shows the energy spectra of 90° equatorial pitch angle electrons and protons between 5 eV to 50 keV. The evolution of these spectra along the ATS 6 geostationary orbit is given as a function of Universal Time for 19 July 1974. Local Times of the satellite are defined by : LT = UT − 0620.

The top panel shows the magnetic field intensity (B, in nT), the B_x component and the inclination angle as measured by a magnetometer along ATS 6 orbit. The corresponding equatorial values of B for McIlwain's M2 magnetic field model are shown for comparison by the solid line in figure 3b [McIlwain, 1972]. It can be seen from the top panel of figure 3a that the observed diurnal variation of B corresponds to undisturbed conditions. The K_p index did not exceed 3- on the day before this observation. It remained low ($K_p \cong 1$ & 2+) from 7/18/74 at 0300 UT till 7/20/74 at 0600 UT, including the period of time corresponding to figure 3a. The photographic density in the two lower panels is a logarithmic function of the particle flux measured with the East/West detectors which are spinning round an axis almost perpendicular to the magnetic field direction.

Note that injected protons and electrons of almost zero energy are detected along the geostationary orbit at the same local time as they would be if they were convected from a common source region towards the position of the satellite. Their drift path between the source and the detectors is determined only by the distribution of $\vec{V}_E = \vec{E} \times \vec{B}/B^2$, the electric drift velocity in the magnetosphere. This electric drift velocity is parallel to the equipotential lines shown in figure 1. Protons with non-zero energies experience an additional westward gradient-B drift.

Uniform injection along the magnetopause

Let us first assume that the magnetopause surface or the Plasma Boundary Layer, is a steady and uniform source of protons and electrons with energies ranging from 0 to 50 keV. In this case the first zero-energy particles drifting inwards from the magnetopause will be detected at 2230 LT where the last closed equipotential intersects the geostationary orbit. This last closed equipotential is the outer boun-

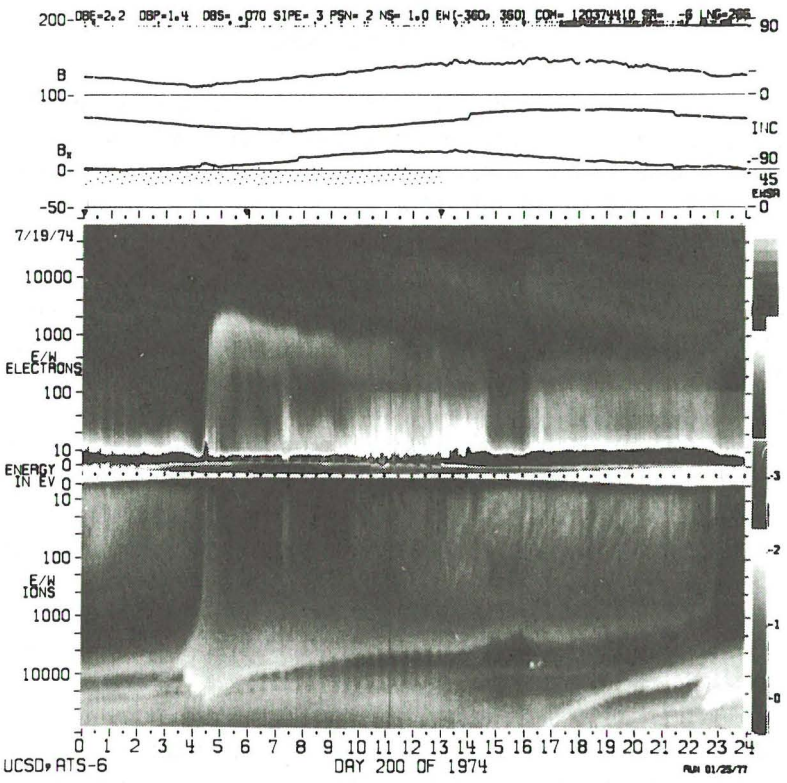

FIG. 3a. — The spectrogram of data from ATS 6 acquired on 19 July 1974. The electron and proton energy spectra have been measured with the plasma spectrometers which are directed nearly perpendicular to the magnetic field direction. The flux intensity is determined by the brightness of the photographic density. Local times and Universal times of the satellite ATS 6 are given respectively by the upper and lower scales. The top panels contain the intensity (B), the B_x component and the Inclination angle of the local magnetic field measured at the position of ATS 6.

dary of the shaded area in figure 1. The geostationary orbit is shown by the dashed line at $R = 6.6\ R_E$.

All zero-energy particles detected after 2230 LT at $R = 6.6$ have either been emitted along the duskside flank of the Plasma Boundary Layer (PBL) after 1710 LT, or they are charged particles drifting down the tail toward the Earth. These zero-magnetic moment particles can be detected until 1044 LT where the last closed equipotential of the E3H field intersects again the geostationary orbit. In the

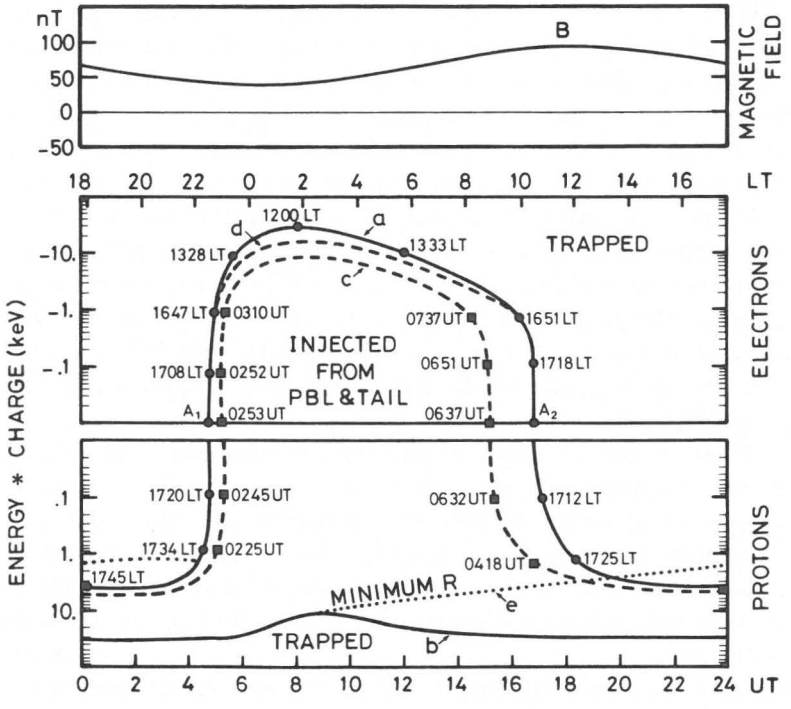

FIG. 3b. — A plot showing the type of particle trajectories encountered by the ATS 6 geostationary satellite according to the E3H and M2 electric and magnetic field models. The scales are the same as in figure 3a.

dynamical spectrogram shown in figure 3b all zero-energy particles drifting inwards from the PBL or from the magnetotail should therefore be observed between points A_1 (2230 LT, 0450 UT) and A_2 (1044 LT, 1704 UT).

After 1044 LT but before 2230 LT trapped zero-energy electrons or protons can come neither directly from Plasma Boundary Layer nor from the magnetotail, but must be of ionospheric origin.

Electrons of higher energy experience an eastward gradient-B in addition to the electric drift velocity $\vec{V}_E$. The gradient-B drift is proportional to the perpendicular energy of the particle. As a consequence the trajectories of electrons with non-zero magnetic moments differ from the streamlines shown in figure 1. The last closed streamline for −0.1 keV/nT electrons intersects the geostationary orbit at

2231 LT and 1031 LT. Particles of this magnetic moment, that have been observed between these two local time limits, must have been emitted at the PBL or have drifted earthwards down from the magnetotail. These local time limits depend on the sign of the electric charge of the particles since the gradient-B drift velocity is eastward for negatively charged particles and westward for positive ions. The upper solid line (a) in figure 3b gives the local time limits between injected and trapped electrons as a function of energy. It can be seen that for electron energies above a certain limit ($\sim$ 30 keV), all trajectories intersecting the geostationary orbit are closed. Any electrons observed along geostationary orbit with an energy greater than 30 keV (in the direction perpendicular to $\vec{B}$) must be particles trapped inside the magnetosphere.

There is also an upper energy limit beyond which all protons detected by ATS 6 at a given LT are on trapped orbits and can never penetrate into either the PBL or the magnetotail. This local time dependent energy limit is shown by the lower solid line (b) in figure 3b. Protons observed at geostationary orbit which have higher energies have not been convected down from the tail, but are westward drifting trapped ions which have been injected at an earlier substorm and form the Ring Current. Note that the position of the solid line (b) is independent of the mass of the ions which are measured.

The numbers given along the line (a) are the local times where the particles have been emitted at the inner edge of the Plasma Boundary Layer. It can be seen that these local times range from 1200 LT to 1745 LT (i.e. the afternoon local time sector); the protons and electrons observed by ATS 6 at 0500 UT with energies below 1 keV are all injected along the magnetopause in a rather narrow range of local times in the later afternoon sector between 1647 LT and 1734 LT. The last Plasma Boundary Layer electrons and protons observed by ATS 6 at 1700 UT with energies below 1 keV have penetrated into the magnetosphere between 1651 LT and 1725 LT (see fig. 3b).

Note the good coïncidence of the line (a) with the sharp S-shaped spectral feature, seen in figure 3a, between 0400 UT and 0500 UT for proton and electron energies below 1 keV. For these low energy particles the electric field distribution in the magnetosphere plays the dominant role, since the gradient-B drift is small for energies smaller than 1 keV. The good agreement between these experimental results

and the model calculation argues for the relevance of the E3H electric field model.

If the whole Plasma Boundary Layer and magnetotail were a steady and uniform source of electrons and protons of all energies, a uniformly distributed by flux would be observed almost everywhere between the solid lines (a) and (b) in the spectrogram of figure 3b. Since this is not the case in figure 3a, one can infer that the source region has a finite extent in local time along the magnetopause flank, i.e. that particles are convected to the geostationary orbit from a rather limited range of local times along the inner edge of the Plasma Boundary Layer.

This is not the only possible interpretation of the feature seen in the spectrogram of figure 3a between 0400 UT and 0500 UT. To check this working hypothesis one would need two or more magnetospheric satellites simultaneously in orbit to measure the proton and electron fluxes between 0 and 50 keV. Until such coordinated and multisatellite observations become available one cannot, however, rule out the interpretation given above.

Patchy injection region at the magnetopause

It can be seen from the spectrograms of figure 3a that the flux of low energy electrons observed at $R = 6.6\ R_E$ is limited within a narrow local time strip. This seems to indicate that the source of the low energy protons and electrons is limited in local time as indicated above. The dashed line (c) in figure 3b gives the Universal Time at which ATS 6 can detect particles which have penetrated across the magnetopause at 1900 LT. These particles have penetrated into the magnetosphere at different Universal Times indicated along the line (c), e.g. a zero-energy particle encountered by ATS 6 at 0525 UT has penetrated into the magnetosphere at 0253 UT in the 1900 Local Time sector along the magnetopause. It can be seen that the particles observed by ATS 6 between 0400 UT and 0600 UT could have been injected into the magnetosphere over a time period extending from before 0225 UT to after 0310 UT.

Between the injection region at the magnetopause and the location of the satellite, the particles have gained kinetic energy because of the change of the electric potential along their drift paths. As a conse-

quence of the conservation of the first adiabatic invariant the perpendicular energy of these particules is proportional to the magnetic field intensity. The magnetic field intensity at their injection point at the magnetopause is 7 nT, while the magnetic field at geostationary orbit is 90 nT. Therefore the energy of a particle detected by ATS 6 with an energy of 1 keV was originally 13 times smaller i.e. 77 eV. In other words, the Betatron acceleration mechanism in the E3H + M2 electric and magnetic field distributions can account for how magnetosheath protons or electrons of 70 eV are able to acquire an energy of 1 keV at geostationary orbit.

Since the highest particle fluxes near 0525 UT are confined within a narrow vertical strip (i.e. only during one hour UT) one can also suggest that the injection region did not extend beyond 1900 LT along the magnetopause or Plasma Boundary Layer.

High energy injected electrons are missing above 5 keV in figure 3a. The maximum observed energies are smaller than those corresponding to the solid line (a). This discrepancy can be partially resolved by further limiting the local time extent of the injection region at the magnetopause. Indeed if this injection region does not extend to local times earlier than 1600 LT, the upper energy limit of injected electrons is lowered from line (a) to line (d) in figure 3b.

From the comparison of figures 3a and 3b, it can be seen that the observed upper limit is still higher than the calculated line (d). Therefore some other or an additional effect needs to be found to resolve the discrepancy. One possible explanation could be that the cloud of injected particles (source region), which has penetrated impulsively into the duskside flanks of the magnetotail did not contain many electrons with initial energies greater than 210 eV which would then have been measured at geostationary orbit with a final energy greater than 5 keV, as a result of the betatron acceleration process. This explanation for the low fluxes of electrons above 5 keV is supported by plasma observations in the magnetosheath which show that the solar wind electron energy spectra are rather depleted above 200 eV.

We have shown that the narrow band of enhanced electron flux observed between 0400 UT and 0525 UT along the ATS 6 trajectory can be accounted for by an injection region initially located along the magnetopause at local times later than 1600 LT and before 1900 LT. This result can be considered as additional evidence for patchy or localized injection of magnetosheath plasma into the magnetosphere

instead of steady-state diffusion or uniformly distributed penetration across the magnetopause.

The satisfactory agreement obtained between the position of this observed S-shaped spectral feature and the low energy portion of the line (a) in figure 3b, indicates that the E3H electric field does indeed fit ATS 6 observations of electrons and protons between 0400 UT and 0600 UT.

The fading of the spectral intensity after 0600 UT within the bright strip feature in the electron spectrogram of figure 3a, may be the consequence of scattering and pitch angle diffusion as the beam of electron proceeds deeper into the magnetosphere.

But it may also be evidence for the slow extinction of the source of injected particles, i.e. for a depletion of the particle reservoir as time proceeds.

Simultaneous observations at different locations would be required to determine how much fading is due to the time variation of the source, and how much is a consequence of continuous scattering of particles penetrating into the deeper region of the magnetosphere.

The deep minimum in the proton spectrum

There are some protons that are injected at the magnetopause and penetrate rather deep into the magnetosphere before they are detected at geostationary orbit. Such westward drifting protons spend their longest time in the denser cold plasma region of the inner magnetosphere where their drift velocity is significantly reduced because of the large magnetic field intensity B. Indeed both the electric and gradient-B drifts are inversely proportional to the magnetic field intensity, B. Therefore these protons could be lost before they traverse the geostationary orbit for the second time. A deep minimum is expected in the proton spectrum for all energies corresponding to the orbits penetrating far inside the geomagnetic field. McIlwain (1972) has shown that the E3 field model predicts the observed position of this minimum in the ATS 5 energy spectra. The dashed line (e) in figure 3b gives the energy for which the penetration in the E3H field is deepest : i.e. the trajectory with the minimum minimorum radial distance. The agreement between the line (e) and the observed minimum in the proton spectrogram of figure 2a, is very satisfactory and is an

additional confirmation of the relevance of the E3H electric field model.

The deep minimum in the proton spectra is most clearly observed between 0000 LT and 1400 LT ; between 2200 LT and 2400 LT the proton flux has a maximum intensity. The intensification during this latter local time interval is observed when the satellite penetrates into the pre-midnight local time sector where it detects the protons coming directly down the magnetotail, before they pass through their deepest penetration point (i.e. before they have been scattered) ; along the rest of geostationary orbit these 10-20 keV protons are measured after passing through lower L-shells.

Instead of using the minimum minimorum radial distance to determine the energy of the deep minimum in the proton spectra, McIlwain [1972] has used two alternative criteria : 1) the maximum maximorum magnetic field intensity and 2) the longest drift time. All three criteria lead to energies for the deep minimum which are close to each other and are sometimes hard to distinguish numerically.

The minimum in the proton spectra is a consistent feature found in most ATS 5 and 6 spectrograms. Any relevant consistent magnetospheric electric and magnetic field models should therefore be able to predict precisely the position of this deep minimum in the proton spectra. The E3H model was carefully tailored to do so [McIlwain, 1972, 1974].

Conclusions

Confirmations for the relevance of McIlwain's electric field model E3H have been obtained using dynamic spectrograms of electrons and protons observed along the geostationary orbit of ATS 6 during an extended period of time when the geomagnetic activity remained low and nearly constant ($K_p \cong 1\text{-}2$). Indeed the positions of the deep minimum observed in the proton energy spectra of figure 3a between 2 keV and 10 keV, correspond to the energy for which these particles penetrate deepest into the magnetosphere when this limit is computed with the E3H model. Furthermore, the S-shaped injection boundary, in figure 3b, separating the trapped electrons from those injected from the Plasma Boundary Layer or from the magnetotail, has been calculated using the E3H model ; the theoretical result fits very precisely the experimental observations made onboard ATS 6 (see fig. 3a).

Although, a fair agreement has been found between the E3H model predictions and ATS 6 observations for a whole 24 hour period when K_p stayed between 1 and 2, it should not be concluded that all spectrograms observed during more disturbed days can be interpreted in terms of this empirical electric field model. Indeed under most of these circumstances, stationary electrostatic field distributions are useless ; time dependent and irregular electric field models should then be used instead of the E3H model, or of any other simpler approximation of the equatorial electric field distribution such as the uniform dawn-dusk model (fig. 2) or Stern-Volland's set of models.

It has been suggested that a localized injection of plasma from a narrow local time sector of the late afternoon Plasma Boundary Layer can explain the narrow band of low-energy electrons and protons (< 1 keV) observed between 0400 UT and 0600 UT in figure 3a. However, such an interpretation is tentative and would need additional experimental confirmation from future coordinated and multi-satellite observations.

ACKNOWLEDGEMENTS

I wish to thank C. E. McIlwain for making the ATS 6 data available to me as well as the computer facilities at the CASS. I would like to thank C. E. McIlwain and E. C. Whipple also for their hospitality when I was visiting at the University of California, San Diego.

REFERENCES

AXFORD, W. I. and HINES, C. O., 1961. A unifying theory of high-latitude geophysical phenomena and geomagnetic storms, *Cand. J. Phys.*, **39**, 1433-1464.

BRICE, N. M., 1967. Bulk motion of the magnetosphere, *J. Geophys. Res.*, **72**, 5193-5211.

CARPENTER, D. L., 1963. Whistler evidence of a knee in the magnetospheric ionization density profile, *J. Geophys. Res.*, **68**, 1675-1682.

CARPENTER, D. L., 1966. Whistler studies of the plasmapause in the magnetosphere. I. Temporal variations in the position of the knee and some evidence of plasma motions near the knee, *J. Geophys. Res.*, **71**, 693-709.

DE FOREST, S. E. and MCILWAIN, C. E., 1971. Plasma clouds in the magnetosphere, *J. Geophys. Res.*, **76**, 3587-3611.

KAVANAGH, L. D., Jr., FREEMAN, J. W., Jr. and CHEN, A. J., 1968. Plasma flow in the magnetosphere, *J. Geophys. Res.*, **73**, 5511-5519.

LEMAIRE, J., 1975. The mechanisms of formation of the plasmapause, *Ann. Géophys.*, **31**, 175-190.

LEMAIRE, J., 1976. Steady state plasmapause positions deduced from McIlwain's electric field models, *J. Atm. Terr. Phys.*, **38**, 1041-1046.

LEMAIRE, J. and KOWALKOWSKI, L., 1981. The role of plasma interchange motion for the formation of a plasmapause, *Planet. Space Sci.*, **29**, 469-478.

MCILWAIN, C. E., 1972. Plasma convection in the vicinity of the geosynchronous orbit, in "*Earth Magnetospheric Processes*", pp. 268–279, ed. B. M. McCormac, D. Reidel Publ. Co., Dordrecht-Holland.

MCILWAIN, C. E., 1974. Substorm injection boundaries, in "*Magnetospheric Physics*", pp. 143-154, ed. B. M. McCormac, D. Reidel Publ. Co., Dordrecht-Holland.

NISHIDA, A., 1966. Formation of plasmapause, or magnetospheric plasma knee, by the combined action of magnetospheric convection and plasma escape from the tail, *J. Geophys. Res.*, **71**, 5669-5679.

STERN, D. P., 1977. Large-scale electric fields in the earth's magnetosphere, *Rev. Geophys. Sp. Phys.*, **15**, 156-194.

VOLLAND, H., 1973. A semiempirical model of large-scale magnetospheric electric fields, *J. Geophys. Res.*, **78**, 171-180.